Simulation of three-dimensional free-form surface normal machining by 3SPS+RRPU and 2SPS+RRPRR parallel machine tools

Y Lu* and **J-Y Xu**
College of Mechanical Engineerig, Yanshan University, Hebei, People's Republic of China

The manuscript was received on 4 May 2007 and was accepted after revision for publication on 11 December 2007.

DOI: 10.1243/09544054JEM900

Abstract: A novel 5-degrees-of-freedom (DOF) 3SPS+RRPU parallel machine tool (PMT) and a novel 5-DOF 2SPS+RRPRR PMT are proposed for a three-dimensional (3D) free-form surface normal machining. A computer aided design (CAD) variation geometry approach is adopted for solving the extension/rotation of linear/rotational actuators and the pose of the two PMTs during machining. First, two simulation mechanisms are created by the CAD variation geometry technique for the 3SPS+RRPU PMT and the 2SPS+RRPRR PMT, respectively. Second, a 3D free-form surface and a guiding plane of tool path are constructed above the moving platform of the simulation mechanism. Third, the tool axis of the simulation PMT is kept normal to the 3D free-form surface, and two 5-DOF simulation PMTs are created. Finally, in the light of the two prescribed tool paths, the extension/rotation of linear/rotational actuators, and the pose of the PMTs are solved automatically and visualized dynamically.

Keywords: computer simulation, parallel machine tool, three-dimensional free-form surface, normal machining

1 INTRODUCTION

Recently, parallel kinematic machines (PKMs) have been studied extensively [**1**, **2**]. PKMs, especially the six-degree-of-freedom (6-DOF) hexapods, possess novel features of closed-loop and symmetrical mechanism, and optimized low moving weight. The hexapod-based parallel machine tool (PMT) has been often credited with high speed, high rigidity, high dynamic bandwidth, high accuracy, and low cost. It has been successfully used to machine a three-dimensional (3D) workpiece [**2**–**4**]. In order to simplify structure and control processes, some limited-DOF PMTs have been developed, such as a 3-DOF tripod machine tool [**5**], a 3-DOF 3-prizmatic-revolute-sperical (3-PRS) serial–parallel machine tool [**6**, **7**], a variax five-axis parallel kinetic machining centre [**8**], a three-axis PMT [**9**, **10**], a high-speed three-axis PMT [**11**, **12**]. In order to improve machining quality, a 3D free-form surface normal machining is required and can be completed by some PMTs with more than 4-DOFs [**2**, **3**]. Fang and Tsai synthesized a class of 5-DOF PKMs by screws theory [**13**]; Li and colleagues synthesized 3R2T 5-DOF PKMs by Lie group of displacements [**14**, **15**]; Gao *et al.* synthesized new kinematic structures for 2–5-DOF PKMs [**16**]; Zhang and Gosselin [**17**] and Alizade and Bayram [**18**] studied some 5-DOF PKMs and *n*-DOF PKMs with a passive constraint leg.

In the traditional milling and computer numerical control (CNC) processes, tool axis is required perpendicular to the 3D free-form surface for improving machining quality. However, it is not easy to compile the NC code for machining a complicated 3D free-form surface, such as a model of an automobile windshield, an impeller blade of a ship, a launch, or a turbine [**12**, **19**–**22**]. Lu proposed a computer aided design (CAD) variation geometric approach for kinematic analysis of some PKMs [**23**–**25**], and successfully simulated the 3D free-form surface vertical machining by 6- or 3-DOF PMTs [**26**–**29**]. Up to now, there has been no effort towards the 3D free-form surface normal machining by 5-DOF

**Corresponding author: College of Mechanical Engineering, Yanshan University, Qinhuangdao, Hebei 066004, People's Republic of China. email: luyi@ysu.edu.cn*

PMTs with fewer than five legs. The current paper focuses on a 3D free-form surface normal machining by a 3SPS+RRPU PTM and a 2SPS+RRPRR PTM. In addition, a novel CAD variation geometry approach is developed for the 3D free-form surface normal machining by this two PMTs without compiling any NC code.

2 THE 3SPS+RRPU PKM AND ITS SIMULATION MECHANISM

2.1 The 3SPS+RRPU PKM and its DOF

A 3SPS+RRPU PKM includes a moving platform m, a fixed base B, and 3 SPS (spherical joint–active prismatic joint-spherical joint) active legs r_i ($i=1,2,3$) with linear actuators, and one central RRPU (active revolute joint–revolute joint–active prismatic joint–universal joint) active leg r_o with a linear actuator and a rotational actuator; see Fig. 1(a) where m is an equilateral ternary link $\Delta a_1a_2a_3$ with three sides $l_i=l$, three vertices a_i, and a centre point o; B is an equilateral ternary link $\Delta A_1A_2A_3$ with three sides $L_i=L$, three vertices A_i, and a centre point O. Let $\{m\}$ be a coordinate system o-xyz fixed on m at o. Let $\{B\}$ be a coordinate system O-XYZ fixed on B at O. $\perp$ and $\|$ denote a perpendicular constraint and a parallel constraint respectively. Each of r_i connects m to B by a spherical joint S at a_i, an active leg r_i with a prismatic joint P, and a spherical joint S at A_i. The central RRPU active leg r_o connects m to B by a universal joint U, a leg r_o with an active prismatic joint P, a revolute R_{B2}, and an active revolute joint R_{B1}. U is attached to m at o, and is composed of two cross revolute joints R_{m1} and R_{m2}. R_{B1} is attached to B at O and is connected with the axis of the motor. R_{B2} and R_{B1} are crossed and connected by a link. Some geometric constraints (R_{B1} and Z being collinear, $R_{B1}\perp R_{B2}$, $R_{m2}\|R_{B2}$, $R_{m1}\perp R_{m2}$, and R_{m1} and x being collinear) are satisfied. Since each of the SPS active legs r_i bears only the axial force along r_i, the 3SPS+RRPU PKM obviously has a relative large capacity of load-bearing.

In the 3SPS+RRPU PKM, the number of links are $k=11$ for one platform, four cylinders, four pistonrods, one link for connecting R_{B1} and R_{B2}, and one base; the number of joints is $g=13$ for four prismatic joints, two revolute joints, one universal joint, and six spherical joints; $f_1=1$ for the prismatic or revolute joint, $f_2=2$ for the universal joint, $f_2=3$ for the spherical joint; the redundant DOF is $F_0=3$ for three SPS-type active legs rotating about their own axes, and F_0 has no influence on the kinematic characteristics. Thus, the DOF F of the 3SPS+RRPU PKM can be calculated by a revised Kutzbach–Grubler equation [**1**] as

$$F=6(k-g-1)+\sum_{i=1}^{g}f_i-F_0$$
$$=6\times(11-13-1)+(4\times1+2+2+6\times3)-3=5$$

2.2 The simulation 3SPS+RRPU PKM

In order to construct a simulation 3SPS+RRPU PMT and verify its DOF, a simulation 3SPS+RRPU PKM (see Fig. 1(b)) is created by CAD variation geometry techniques of some CAD softwares such as SolidWorks, Solid-Edge, Solid-Designer, Mechanical Desktop, Pro/E, and so on. Some basic techniques of CAD variation geometry techniques for constructing simulation mechanisms and verifying the DOF of

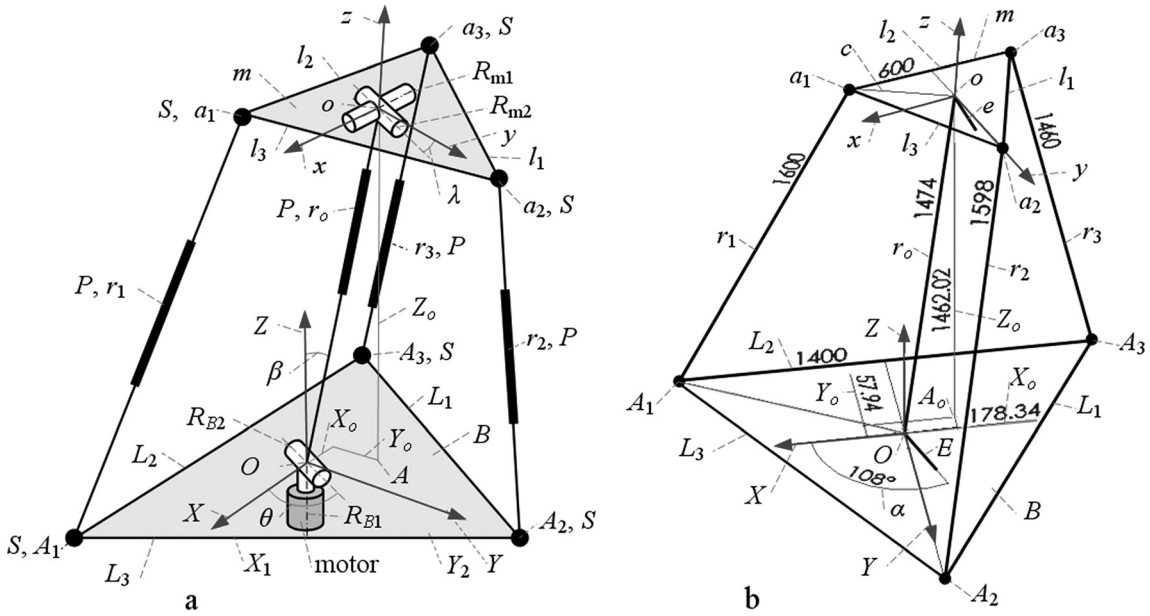

Fig. 1 The 3SPS+RRPU PKM and its simulation mechanism

the PKM are described in Appendix 2 and references [**23**], [**28**], and [**29**].

The creation procedures of the simulation 3SPS+RRPU PKM are outlined below.

1. Construct the base B in a two-dimensional sketch. The sub-procedures are:
   (a) construct an equilateral triangle $\Delta A_1A_2A_3$ by the polygon command;
   (b) coincide its centre point O with origin of default coordinate, set its one side horizontally, and give its one side a fixed dimension in length;
   (c) transform $\Delta A_1A_2A_3$ into a plane by the planar command.
2. Construct the platform m in a 3D sketch. The sub-procedures are:
   (a) create three lines l_i ($i=1, 2, 3$), and connect them to form a closed triangle $\Delta a_1a_2a_3$;
   (b) give each of l_i the same initial dimension;
   (c) create a line y, and connect its two ends to a_2 and l_2; (d) create a line c, and connect its two ends to a_1 and y at point o;
   (e) set $y \perp c$ and $c \perp l_2$.
3. Construct three SPS-type active legs. The sub-procedures are:
   (a) construct three lines r_i ($i=1, 2, 3$), and connect their two ends to m at a_i and to B at A_i by the point-to-point coincident constraint;
   (b) give each of r_i the initial driving dimension in length for linear actuators.
4. Construct a RRPU-type active leg. The sub-procedures are:
   (a) construct a line r_o, and connect its two ends to m at o and to B at O;
   (b) construct an auxiliary line E for two crossed revolute joints R_{B1} and R_{B2}, and connect its one end to B at O;
   (c) construct an auxiliary line e for the universal joint U, and connect its one end to m at o;
   (d) set $E \perp Z$, $e \perp l_2$, $r_o \perp e$, $r_o \perp E$, and $e \| E$;
   (e) give the angle θ between line E and line L_2 a driving dimension for the rotational actuator of R_{B1}, and give line r_o a driving dimension in length for the linear actuator.

Thus, a simulation 3SPS+RRPU PKM is constructed.

The pose of m in $\{B\}$ can be solved by the procedures outlined below.

1. Construct a line Z_o, connect its two ends to m at o and to B at point A_o, and set $Z_o \perp B$. Construct a line z_1, connect its one end to B at O and set $z_1 \perp m$.
2. Take the default coordinate O-XYZ as a fixed coordinate on B, give each of the distances from A_o to Y, X, and o the driven dimensions respectively. Give the angles (α, β, γ) between z_1 and X, Y, Z the driven dimensions respectively.
3. When varying the driving dimensions of (r_o r_1 r_2 r_3 θ), the pose parameters (X_o, Y_o, Z_o, α, β, γ) of m in $\{B\}$ are solved automatically and visualized dynamically. Therefore, it is verified that the 3SPS+RRPU PKM has five DOFS.

3 3SPS+RRPU PMT AND ITS SIMULATION MECHANISM

3.1 The guiding plane P_0 of tool path and 3D free-form surface s

When a tool T, such as a milling cutter or a grounding wheel, is installed perpendicularly onto the platform m of the 3SPS+RRPU PKM, a 3SPS+RRPU PMT is formed. When a 3D free-form surface s and a guiding plane P_0 of the tool path are attached on B above m of the simulation mechanism, and T is kept perpendicular to s at any point, a simulation 3SPS+RRPU PMT is created; see Fig. 2. Before creating simulation PMT, the guiding plane P_0 and 3D free-form surface s must be created by the 3D modelling technique. How to fix s and P_0 on B of PMT and arrange them above m of PMT is a key issue to be solved. A guiding plane P_0 of the tool path and a 3D free-form surface s are created as follows.

1. Modify B of the simulation mechanism, and construct a datum plane P_0 by the reference plane command. Set $P_0 \| B$, and give the distance from P_0 to B a fixed dimension $h=3000$ mm. Construct a rectangle on P_0, and transform it into a guiding plane of the tool path by the plane-forming command; see Fig. 2.
2. Modify B of the simulation mechanism, construct several datum planes (P_j, $j=1, 2,\ldots k$), and set them parallel to each other and perpendicular to B by the reference plane command.
3. Based on the prescribed curve data or curve equation, construct a spline u_j on the jth plane P_j ($j=1, 2,\ldots k$) by the sketching spline command or data table, and arrange each spline curve with respect to P_0 above m of the simulation mechanism; see Fig. 2(a).
4. Construct a smooth and continuous 3D free-form surface s from all u_j ($j=1, 2,\ldots k$) by some special modelling techniques, such as loft, swept, extrude, rotation commands, etc. Here, s is constructed by a loft modelling technique and attached on B above m and under P_0; see Figs 2 and 3(b) (later).

3.2 The simulation 3SPS+RRPU PMT

Generally, there are two kinds of tool path for machining s. One is a linear reciprocation tool path; the other is a rectangle or circle spiral tool

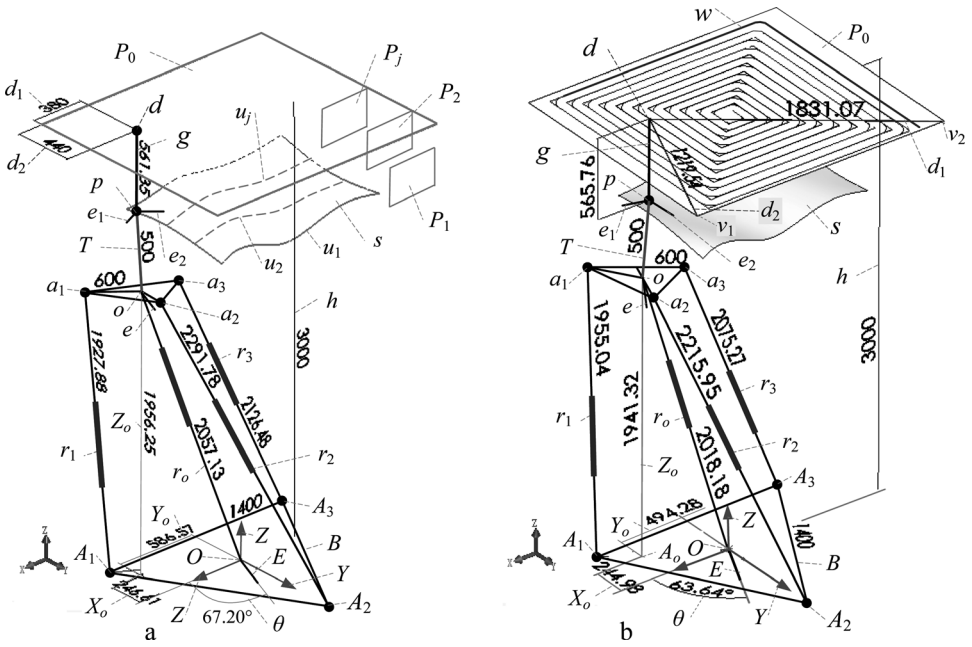

Fig. 2 Two configurations of the simulation 3SPS+RRPU PMT to machine *s* (a) along a linear reciprocation tool path, and (b) along a rectangle spiral tool path

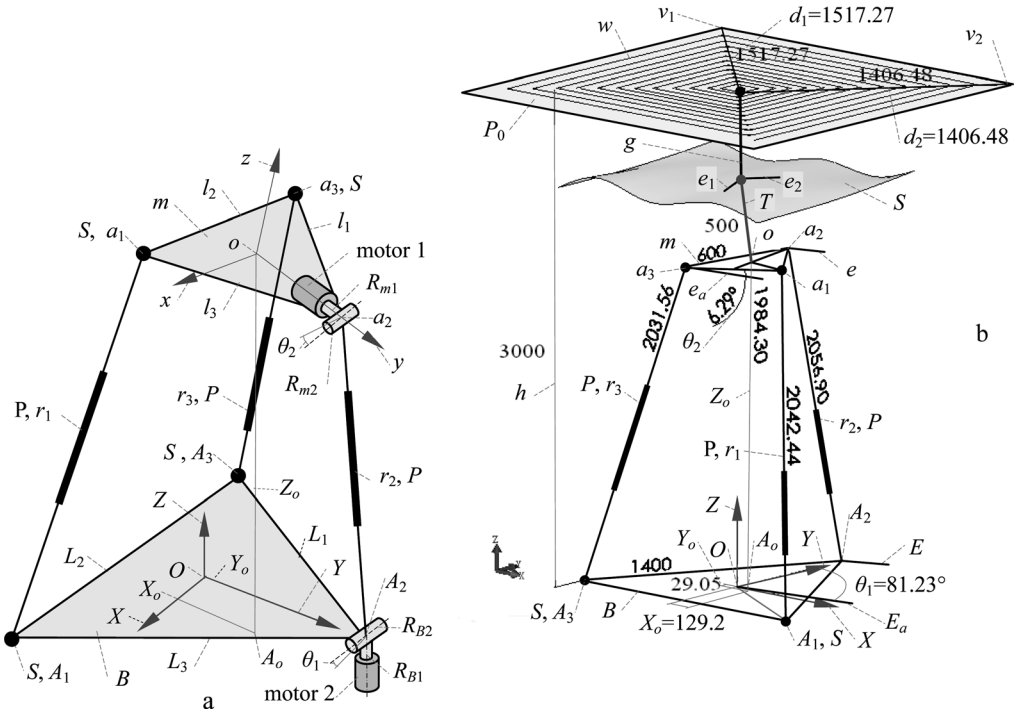

Fig. 3 The 2SPS+RRPRR PKM and its simulation PMT

path. Based on the simulation 3SPS+RRPU PKM in Fig. 1(b), a simulation 3SPS+RRPU PMT with a linear reciprocation tool path for machining *s* is created; see Fig. 2(a).

The creation procedures are outlined below.

1. Transform all the driving dimensions of extension/rotation (r_1, r_2, r_3, r_o, θ) of the linear/rotational actuators in the simulation 3SPS + RRPU PKM into the driven dimensions by the dimension command, and give each of (r_1, r_2, r_3, r_o, θ) a dimension name.
2. Coincide the tip of *T* with *s* at point *p* by the coincident constraint command.
3. Construct a guiding line *g*, connect its two ends to *s* at point *p* and to P_0 at point *d* respectively,

by the coincident constraint command, and set $g \perp P_0$.

4. Construct two short lines e_1 and e_2, connect their one ends to point p, set e_1 and e_2 tangent to s at p, and set $e_1 \perp e_2$, $T \perp e_1$, $T \perp e_2$ by the geometric constraint command. Thus, a geometric constraint $T \perp s$ at p is always satisfied.
5. Give each of the distances from d to the left side and the lower side of P_0 a driving dimension d_1 and d_2 respectively. When varying the driving dimensions of d_1 and d_2, the driven dimensions of the active legs r_o, r_i, rotational angle θ are varied automatically.

3.3 Machining *s* by PMT along a linear reciprocation tool path

When a linear reciprocation tool path w on P_0 is used to machine s, see Fig. 2(a), its constitution procedures are described as follows.

1. Determine the machining range ($d_{y\min}$, $d_{x\min}$, $d_{y\max}$, $d_{x\max}$) and the feed rate (δ_x, δ_y) for each increment. Set $d_{y\min} = d_{x\min} = 300$, $d_{y\max} = 1500$, $d_{x\max} = 1400$ mm, increment $\delta = \delta_x = \delta_y = 10$ mm.
2. Retain $d_2 = d_{y\min}$, and gradually increase d_1 by δ_x each time from $d_{x\min}$ to $d_{x\max}$ by the dimension automatic fill command.
3. Retain $d_1 = d_{x\max}$, and gradually increase d_2 by δ_y each time from $d_{y\min}$ to $d_{y\min} + n_1\delta_y$, $n_1 = 2$.
4. Retain $d_2 = d_{y\min} + n_1\delta_y$, and gradually decrease d_1 by $-\delta_x$ each time from $d_{x\max}$ to $d_{x\min}$.
5. Repeat steps 2 to 4 above, until $d_2 = d_{y\max}$ and $d_1 = d_{x\max}$.

3.4 Machining *s* by PMT along a rectangular spiral tool path

When a rectangular spiral tool path w on P_0 is used in the simulation 3SPS+RRPU PMT, see Fig. 2(b), the machining procedures are described as follows.

1. Construct a set of vertical and horizontal lines on P_0, connect them to form a rectangular spiral curve on P_0, and transform it into a rectangular spiral spline w without any split points.
2. Coincide the free end point d of guiding line g with w.
3. Construct two driving lines d_1 and d_2, and connect their one end to point p and the other end to the two vertices (v_1, v_2) of plane P_0 respectively.
4. Give d_1 and d_2 a driving dimension or a driven dimension alternately, and gradually vary d_2 or d_1 by using the automatic fill function to move d outwards along w. The sub-steps are:
   (a) give d_2 and d_1 a driving dimension and a driven dimension respectively, and gradually vary the driving dimension of d_2 by using the automatic fill function to move d outwards along w from the middle of one line to the middle of the next line;
   (b) give d_2 and d_1 a driven dimension and a driving dimension respectively, and gradually vary the driving dimension of d_1 by using the automatic fill function to move d outwards along w from the middle of one line to the middle of the next line; see Fig. 2(b) and Fig. 3(b).
5. Repeat step 4 until the required machining of s is finished.

4 A 2SPS+RRPRR PKM AND ITS SIMULATION PMT

A 2SPS+RRPRR PKM is similar to the 3SPS+RRPU PKM except that the central RRPU active leg r_o is deleted, and the SPS active leg r_2 is replaced by a new RRPRR (active revolute joint–revolute joint–active prismatic joint–revolute joint–active revolute joint) active leg r_2 with two rotational actuators and one linear actuator; see Fig. 3(a). The RRPRR active leg r_2 connects m to B by an active revolute joint R_{m1}, a revolute joint R_{m2}, a leg r_2 with an active prismatic joint P, a revolute joint R_{B2}, and an active revolute joint R_{B1}. Where, R_{m1} is attached to m at a_2 and connected with the motor 1. R_{B1} is attached to B at A_2 and connected with the motor 2. R_{m1} and R_{m2} are crossed and connected by a link. R_{B1} and R_{B2} are crossed and connected by a link. In addition, some geometric constraints are satisfied: $R_{B1} \perp B$, $R_{B1} \perp R_{B2}$, $R_{m2} \perp r_2$, $R_{m2} \| R_{B2}$, $R_{m1} \perp R_{m2}$, R_{m1} and y being collinear. Since there are only three active linear active legs, the 5-DOF 2SPS+RRPRR PKM is obviously simple in structure.

In the 2SPS+RRPRR PKM, the number of links are $k = 10$ for one platform, three cylinders, three piston-rods, two links, and one base; the number of joints is $g = 11$ for three prismatic joints, four revolute joints, and four spherical joints; the redundant DOFs is $F_0 = 2$ for two SPS active legs rotating about their own axes, and F_0 has no influence on the kinematic characteristics of the PKM. Therefore, the DOFs F of the 2SPS+RRPRR PKM is calculated as

$$F = 6(k-g-1) + \sum_{i=1}^{g} f_i - F_0 = 6\times(10-11-1) + (3\times1 + 2 + 2 + 4\times3) - 2 = 5$$

A simulation 2SPS+RRPRR PKM is similar to the simulation 3SPS+RRPU PKM, except that some additional creation procedures are conducted as follows.

1. Delete the central RRPU active leg r_o of the latter.
2. Transform a SPS active leg r_2 of the latter into a RRPRR active leg r_2. The sub-procedures are:
   (a) create two auxiliary lines E and E_a for revolute joints R_{B1} and R_{B2}, connect their one end to B at A_2 and O respectively;

(b) create two auxiliary lines e and e_a for revolute joints R_{m1} and R_{m2}, and connect their one end to m at a_2 and a_3 respectively;
(c) set $E \perp Z$, $e \perp y$, $E \| E_a$, $e \| e_a$, $r_2 \perp e$, and $r_2 \perp E$;
(d) give an angle θ_1 between line E_a and line Y a driving dimension for motor 2, give a line r_2 a driving dimension in length for a linear actuator, and give an angle θ_2 between line l_3 and line e_a a driving dimension for motor 1.

Thus, a simulation 2SPS+RRPRR PKM is constructed.

Similarly, the pose of m with respect to B can be solved as follows: when varying the driving dimensions of (θ_1, θ_2, r_1, r_2, r_3), the pose parameters (X_o, Y_o, Z_o, α, β, γ) of m in $\{B\}$ are solved automatically. Therefore, it is verified that the 2SPS+RRPRR PKM has 5 DOFs.

Based on the simulation 2SPS+RRPRR PKM, a novel simulation 2SPS+RRPRR PMT is created for a 3D free-form surface normal machining along the rectangle spiral tool path; see Fig. 3(b). Similarly, a simulation 2SPS+RRPRR PMT is created for s normal machining along a linear reciprocation tool path.

5 SIMULATION RESULTS OF 3D FREE-FORM SURFACE NORMAL MACHINING

Since a 3D free-form surface s is smooth and continuous, and may be any prescribed free-form surface, no specified parameters of the 3D free-form surface are given in this example. When varying the driving dimensions of d_1 and d_2, the tool T is moved and retained perpendicular to s at any point. At the same time, the driven dimensions of the active legs in length and rotational angle of motor and the pose parameters (X_o, Y_o, Z_o, α, β, γ) of the simulation 3SPS+RRPU PMT are solved automatically and visualized dynamically by the Excel Table and the configuration function of CAD software; see Fig. 4.

Similarly, the driven dimensions of the active legs in length and rotational angles of two motors and the pose parameters (X_o, Y_o, Z_o, α, β, γ) of the simulation 2SPS+RRPRR PMT are solved automatically; see Fig. 5.

When machining 3D free-form surface s by the simulation 3SPS+RRPU PMT along a linear reciprocation tool path, the extension r_i ($i = 1, 2, 3$) of active legs and the position components (X_o, Y_o, Z_o) of platform versus time are solved; see Fig. 4(a); the angle θ of the rotational actuator and the orientation components (α, β, γ) of platform versus time are solved; see Fig. 4(b).

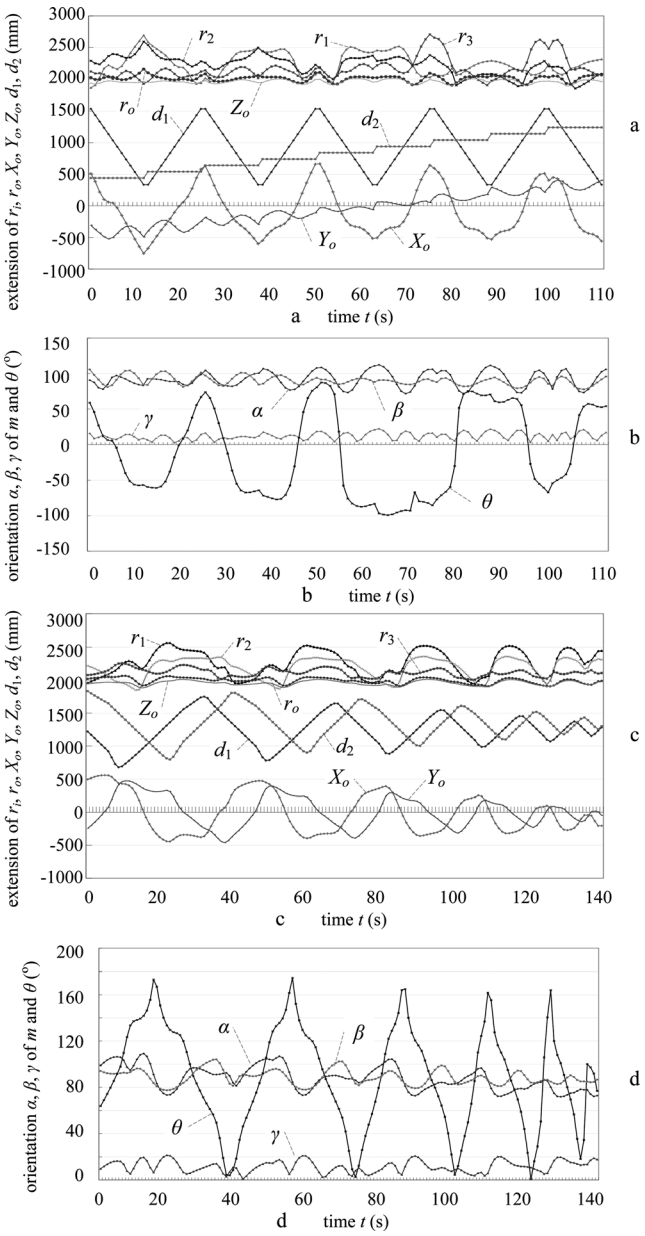

Fig. 4 The simulation results of the simulation 3SPS+RRPU PMT (a) and (b) along a linear reciprocation tool path, and (c) and (d) along a rectangle spiral, tool path

When machining s by the simulation 3SPS+RRPU PMT along a rectangle spiral tool path, the extension r_i ($i = 1, 2, 3$) of active legs and the position components (X_o, Y_o, Z_o) of platform versus time are solved; see Fig. 4(c); the angle θ of the rotational actuator and the orientation components (α, β, γ) of platform versus time are solved; see Fig. 4(d).

When machining s by a simulation 2SPS+RRPRR PMT along a linear reciprocation tool path, the extension r_i ($i = 1, 2, 3$) of active legs and the position components (X_o, Y_o, Z_o) of platform versus time are solved;

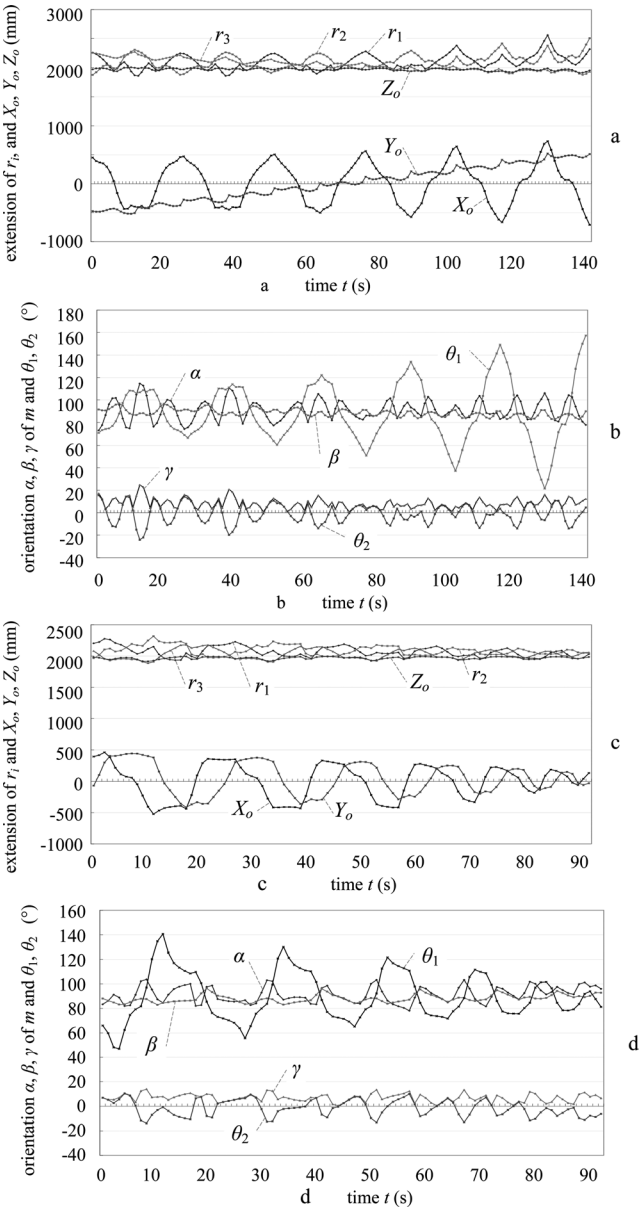

Fig. 5 The simulation results of the simulation 2SPS+RRPRR PMT (a) and (b) along a linear reciprocation path, and (c) and (d) along a rectangle spiral tool path

see Fig. 5(a); the angle θ_1 of rotational actuator 1, the angle θ_2 of rotational actuator 2, and the orientation components (α, β, γ) of the platform versus time are solved; see Fig. 5(b).

When machining s by the simulation 2SPS+RRPRR PMT along a rectangular spiral tool path, the extension r_i ($i = 1, 2, 3$) of active legs and the position components (X_o, Y_o, Z_o) of platform versus time are solved; see Fig. 5(c); the angle θ_1 of rotational actuator 1, the angle θ_2 of rotational actuator 2, and the orientation components (α, β, γ) of platform versus time are solved; see Fig. 5(d).

6 SOME SPECIAL TECHNIQUES OF 3D FREE-FORM SURFACE NORMAL MACHINE

6.1 Machining larger area 3D free-form surface

Generally, the workspace of m is limited by the extent of the linear actuator [**3**, **4**]. When the area of the 3D free-form surface s is larger than the workspace, the extra part of s must be moved into the workspace. For this reason, the position of s in X and Y directions should be varied gradually by the dimension command until the extra part of s is moved into the workspace. Meanwhile, retain the original necessary geometric constraints, such as tool T perpendicular to s, the guideline g perpendicular to the guiding plane P_0, P_0 parallel with the base B, the surface-point coincident between s and the end point p of T, the curve-point coincident between w and the end point d of g, the fixed distance from P_0 to B, the fixed dimension of tool T in length, and all of the geometric constraints of simulation mechanism.

6.2 Combining some simple machining processes

In general, the whole process of machining s should be divided into several subprocesses, such as the tool entering into the machining position, the tool retreating from the machining position, rough machining, rough finishing, and finish machining. For this purpose, the feeding depth of the tool must be varied. Therefore, by only varying the dimension of tool T in length, the issue of feeding normal to s can be solved. In order to complete every submachining process, the following need to be completed.

1. When starting machining, tool T of PMT must be moved from a preparing position to a machining position. Therefore, give T an increment δz at each step from $z_{\min}$ to $z_{\max}$ by using the dimension command for its feeding operation. Next, solve all driven dimensions of driving limbs and pose of m for each step.
2. When completing machining, T must be retreated from s to a suitable position. Therefore, give T an increment δz at each step from $z_{\max}$ to $z_{\min}$ by using the dimension command for its retreating operation, and solve all driven dimensions of driving limbs and pose of m for each step.
3. During rough machining, rough finishing, and finish machining, T must be moved into s at the different depth. For this purpose, the dimension of T should be reduced at the different increment δT in length for different machining processes.
4. Combine all solved data in all subprocesses together, produce a whole machining data.

6.3 Inspecting and avoiding interference

When machining s by PMT, the interference among the active legs and tool path can be checked in the CAD software. For instance, when the simulation 3SPS+RRPU PMT is closed to its initial configuration (i.e. z coincides with Z and $l_i \| L_i$), if an increment of the driving dimensions of d_1 and d_2 is quite small, the platform rotational angle increases greatly, and interference among r_i and r_o may occur. However, when given a larger increment of d_1 and d_2, the platform rotational angle increases little, and interference among r_i and r_o can be avoided.

From the simulation curves, the workspace of PKM can be constructed, then the position of s in respect to platform m can be determined. When the interferences occur, the tool path or PMT can be varied or modified. If a tool path is not suitable for machining s, its size, covered area, position, and path density can be modified by varying the dimensions of the start point and the end point of the tool path on P_0 in respect to B. Thus, a tool path can be used repeatedly.

7 CONCLUSIONS

A novel 5-DOF 3SPS+RRPU PMT (parallel machine tool) has three SPS (spherical joint–active prismatic joint–spherical joint) active legs and one RRPU (active revolute joint–revolute joint-active prismatic joint-universal joint) active leg and has relative large capacity of load bearing. A novel 5-DOF 2SPS+ RRPRR PMT has two SPS active legs and one RRPRR (active revolute joint–revolute joint–active prismatic joint–revolute joint–active revolute joint) active leg and is simple in structure. They can be used for any smooth and continuous 3D free-form surface normal machining of normal lettering or complicated letters on a 3D free-form surface.

Using advanced CAD software, any prescribed 3D free-form surface can be constructed from several precision splines. Based on the 3D free-form surface, the driven dimensions of the driving limbs and the pose of the moving platform of two PMTs can be solved automatically. The simulation solved results of active legs and pose of platform of two PMTs can be transformed into NC codes easily. This approach is straightforward and simple.

A complicated process of machining a 3D free-form surface can be divided into several simple processes to produce its corresponding simulation data. These simulation data in each simple process are used as orderly input into the driving limbs, so that the complicated machining process can be simulated easily.

The kinematic curve of the moving platform can be used to check the workspace of the moving platform and to inspect any interference. By comparing the actual workspace and the simulation workspace of the moving platform, the desired size and location of the workpiece in the two simulation PMTs can be determined.

ACKNOWLEDGEMENTS

The authors would like to acknowledge the financial support of the Natural Sciences Foundation Council of China (NSFC) 50575198.

The authors would like to acknowledge the financial support of a Doctoral Fund from National Education Ministry No. 20060216006

REFERENCES

1 **Huang, Z.** and **Fang, Y. F.** *Mechanism theory of spatial parallel robot and control*, 1998 (Mechanical Industry Press, Beijing, China).
2 **Zhang, S.** and **Heisel, U.** *Parallel machine tool*, 2003 (Mechanical Industry Press, Beijing, China).
3 **Terrier, M., Dugas, A.,** and **Hascoët, J.-Y.** Qualification of parallel kinematics machines in high-speed milling on free form surfaces. *Int. J. Mach. Tools Mf.*, 2004, **44** (7–8), 865–877.
4 **Patel, A. J.** and **Ehmann, K. F.** Calibration of a hexapod machine tool using a redundant leg. *Int. J. Mach. Tools Mf.*, 2000, **40**(4), 489–512.
5 **Chen, J.-S.** and **Hsu, W.-Y.** Design and analysis of a tripod machine tool with an integrated Cartesian guiding and metrology mechanism. *Precision Engng*, 2004, **28**(1), 46–57.
6 **Wang, H.** and **Fan, K.-C.** Identification of strut and assembly errors of a 3-PRS serial–parallel machine tool. *Int. J. Mach. Tools Mf.*, 2004, **44**(11), 1171–1178.
7 **Fan, K.-C., Wang, H., Zhao, J.-W.,** and **Chang, T.-H.** Sensitivity analysis of the 3-PRS parallel kinematic spindle platform of a serial-parallel machine tool. *Int. J. Mach. Tools Mf.*, 2003, **43**(15), 1561–1569.
8 **Geldart, M., Webb, P., Larsson, H., Backstrom, M., Gindy, N.,** and **Rask, K.** A direct comparison of the machining performance of a variax 5 axis parallel kinetic machining centre with conventional 3 and 5 axis machine tools. *Int. J. Mach. Tools Mf.*, 2003, **43**(11), 1107–1116.
9 **Company, O.** and **Pierrot, F.** Modeling and design issues of a 3-axis parallel machine-tool. *Mech. Mach. Theory*, 2002, **37**(11), 1325–1345.
10 **Cai, G. Q., Wang, Q. M., Hu, M., Kang, M. C.,** and **Kim, N. K.** A study on the kinematics and dynamics of a 3-DOF parallel machine tool. *J. Mater. Process. Technol.*, 2001, **111**(1–3), 269–272.

11 **Dong, J., Yuan, C., Stori, J. A.,** and **Ferreira, P. M.** Development of a high-speed 3-axis machine tool using a novel parallel-kinematics X–Y table. *Int. J. Mach. Tools Mf.*, 2004, **44**(12–13), 1355–1371.

12 **Kim, B. H.** and **Choi, B. K.** Guide surface based tool path generation in 3-axis mill: an extension of the guide plane method. *Computer-Aided Des.*, 2000, **32**(3), 191–199.

13 **Fang, Y.** and **Tsai, L.-W.** Structure synthesis of a class of 4-dof and 5-dof parallel manipulators with identical limb structures. *Int. J. Robotics Res.*, 2002, **21**(9), 799–810.

14 **Li, Q.-C., Huang, Z.,** and **Hervé, J.-M.** Type synthesis of 3R2T 5-dof parallel mechanisms using Lie group of displacements. *IEEE Trans. Robotics Automat.*, 2004, **20**(2), 173–180.

15 **Li, Q.-C.** and **Huang, Z.** Mobility analysis of a novel 3-5R parallel mechanism family. *ASME J. Mech. Des.*, 2004, **126**(1), 79–82.

16 **Gao, F.** New kinematic structures for 2-, 3-, 4- and 5-dof parallel manipulator designs. *Mech. Mach. Theory*, 2002, **37**(11), 1395–1411.

17 **Zhang, D.** and **Gosselin, C. M.** Kinetostatic modeling of N-DOF parallel mechanisms with a passive constraining leg and prismatic actuators. *ASME J. Mech. Des.*, 2001, **123**(3) 375–384.

18 **Alizade, R. I.** and **Bayram, C.** Structural synthesis of parallel manipulators. *Mech. Mach. Theory*, 2004, **39** (8), 857–870.

19 **Kim, T.** and **Sarma, S. E.** Toolpath generation along directions of maximum kinematic performance; a first cut at machine-optimal paths. *Computer-Aided Des.*, 2002, **34**(6), 453–468.

20 **Koparkar, P. A.** and **Mudur, S. P.** Generation of continuous smooth curves resulting from operations on parametric surface patches. *Computer-Aided Des.*, 1986, **18**(4), 193–206.

21 **Farin, G.** *Curves and surfaces for computer-aided geometry for design*, 1990 (Academic Press, San Diego. CA, USA).

22 **Hartley, P. J.** and **Judd, C. J.** Parameterization and shape of B-spline curve for CAD. *Computer-Aided Des.*, 1980, **12**(5), 235–238.

23 **Lu, Y.** Using CAD functionalities for the kinematics analysis of spatial parallel manipulators with 3-, 4-, 5-, 6-linearly driven limbs. *Mach. Mech. Theory*, 2004, **39**(1), 46–60.

24 **Lu, Y.** Using CAD variation geometry for solving velocity and acceleration of parallel manipulators with 3-5 linear driving limbs. *Trans. ASME J. Mech. Des.*, 2006, **128**(4), 738–746.

25 **Lu, Y.** CAD variation geometry and analytic approach for solving kinematics of a novel 3-SPU/3-SPU parallel manipulator. *Trans. ASME J. Mech. Des.*, 2006, **128**(3), 574–580.

26 **Lu, Y.** Computer simulation applied to an orthogonal three-rod machine tool for machining a complicated three-dimensional surface. *Int. J. Mach. Tool Mf.*, 2002, **42**(11), 1277–1284.

27 **Lu, Y.** and **Tatu, L.** Computer simulation approach to machining complicated shape on orthogonal 6-rod machine tool. *Int. J. Mach. Tool Mf.*, 2002, **42**(4), 441–447.

28 **Lu, Y.** Computer-aided geometric machining of a 3D free surface using a 3-UPU spatial parallel machine tool. *Int. J. Advd Mf. Technol.*, 2005, **26**(10), 1018–1025.

29 **Lu, Y.** and **Xu, J.** Computer simulation machining a 3D free surface by using a 3-RPRU parallel machine tool. *Int. J. Advd Mf. Technol.*, 2007, **33**(7–8), 782–792.

APPENDIX 1

Notation

B	base
c_i	binary link $i = 1, 2, \ldots, 6$
d_1, d_2	two driving dimensions
F	numbers of degree of freedom
F_0	local redundant degree of freedom
g	guiding line of tool
l_i	sides of m
L	sides of base B
m	moving platform
o	central point of m
O	central point of base
p	tip of tool
P	prismatic joint
P_j	datum plane for sketching spline u_j
P_0	guiding plane of tool path curve
PKM	parallel kinematic machine
PMT	parallel machine tool
r_i	active legs $i = 0, 1, 2, 3$ or its length
R	revolute joint
s	three-dimensional free-form surface
S	sphere joint
T	cutter tool
u_j	prescribed spline on P_j, $\quad j = 1, 2, \ldots k$
U	universal joint
w	prescribed tool path curve
X_o Y_o, Z_o	three position components of m
α, β, γ	three orientation components of T
θ, θ_1, θ_2	active angles of rotational actuators
$\perp$	perpendicular constraint
$\parallel$	parallel constraint

APPENDIX 2

Some basic techniques of CAD geometric variation techniques are explained.

1. The dimensions in the simulation mechanism are classified into the driving dimension, the driven dimension, and the fixed dimension. The driving dimensions are given to the driving limbs for driving m to move. The driven dimensions are given to the pose of m in the respect to B for

solving kinematic parameters of mechanism. The fixed dimensions are given to the sideline of m and B for modifying the size and configuration of the simulation mechanism.

2. Construct a line, when giving it a fixed dimension, a driving dimension, and a driven dimension, the line is equivalent a binary link, an active leg with prismatic joint P and a passive constraint leg with prismatic joint P, respectively.
3. Construct a line and a link, connect the one end of line to any vertex point of link (such as B, m, and another line) by the point–point coincident command. Thus, the connecting point is equivalent to a spherical joint S.